DOE/ER/13649--5

DE92 004423

MECHANISMS OF GAS PERMEATION THROUGH POLYMER MEMBRANES

(Contract No. DE-EG02-87ER 13649)

SUMMARY TECHNICAL REPORT

for Period September 1989 - August 1991

by

S. Alexander Stern

Dept. of Chemical Engineering and Materials Science

Syracuse University, Syracuse, NY 13244

(315) 443-4469

Prepared for:

U.S. DEPARTMENT OF ENERGY

OFFICE OF BASIC ENERGY SCIENCES

TABLE OF CONTENTS

MECHANISMS OF GAS PERMEATION THROUGH POLYMER MEMBRANES

I. INTRODUCTION

The objective of the present study is to investigate the mechanisms of gas transport in and through polymer membranes and the dependence of these mechanisms on pressure and temperature. This information is required for the development of new, energy-efficient membrane processes for the separation of industrial gas mixtures (1,2). Such processes are based on the selective permeation of the components of gas mixtures through **nonporous** polymer membranes.

Recent work has been focused on the permeation of gases through membranes made from **glassy** polymers, i.e., at temperatures below the glass transition of the polymers (Tg). Glassy polymers are very useful membrane materials for gas separations because of their high selectivity toward different gases.

Gases permeate through nonporous polymer membranes by a "solution-diffusion" process (1-5). Consequently, in order to understand the characteristics of this process it is necessary to investigate also the mechanisms of gas solution and diffusion in glassy polymers. During the past report period considerable progress has been made in three areas:

1) A new model of gas solubility in glassy polymers based on a "concentration-temperature superposition principle" has been validated by additional experimental data. This model makes use of a modified Doolittle equation (6) and is particularly useful in cases where the polymer is significantly plasticized (swelled) by the penetrant gas. The Doolittle equation has been used extensively by other investigators to describe and correlate **viscoelastic** phenomena in

polymers(7).

2) The "concentration-temperature superposition principle" has been successfully extended to the **diffusion** of gases in polymers and the **permeation** of gases through polymer membranes. Good agreement has been obtained between theory and experimental data reported in the literature. The new model permits the prediction of the permeation "time-lag" in glassy polymers.

3) The factors responsible for the differences in the gas permeability and selectivity of **meta** and **para** isomers of polyimides have been identified. The meta isomers always exhibit a lower permeabilty and higher selectivity than the para isomers. Dynamic mechanical analyses and theoretical calculations indicate that this behavior is due to differences in the intrasegmental mobility of the polymer chains. Polyimides are presently being investigated in a number of laboratories as potentially useful materials for the removal of acid gases (CO_2 and H_2S) from natural gas, the separation of air, and the separation of H_2 from various industrial gas streams.

II. THE CONCENTRATION-TEMPERATURE SUPERPOSITION PRINCIPLE

A. Gas Solubility

It is well known that the solubility of gases in glassy polymers is a strongly nonlinear function of the gas pressure. Thus, isothermal plots of the gas concentration c (the solubility) in glassy polymers versus the pressure p at solution equilibrium are commonly concave to the pressure axis. When the polymers are **plasticized** (swelled) by the penetrant gas, the isotherms exhibit an inflection point at some sufficiently high pressure and become linear as the pressure is further increased. Moreover, the linear segment of the solubility isotherms extrapolates to the

origin of the c versus p plots, cf. Figure 1.

The nonlinear segment of such a solubility (sorption) isotherm can be described satisfactorily by a "dual-mode sorption" model (1-4, 8-13). However, this model assumes that the polymer is not significantly plasticized by the penetrant. Our new model describes quantitatively the entire isotherm, including its inflection point and linear section, by means of the equation (6):

$$c = S(0)\ \alpha_T(c) \cdot p\ , \tag{1}$$

where S(0) is a solubility coefficient in the Henry's law limit ($c \rightarrow 0$), and $\alpha_T(c)$ is a "concentration shift factor" defined by the relation:

$$log\ \alpha_T(c) = A\left[\frac{Tg\ (c)\ [Tg(c) - Tg(0)]}{[Tg(0)]^2}\right][Tg(0) - T]\ , \tag{2}$$

where A is a characteristic constant; T is the absolute temperature; Tg(0) is the glass-transition temperature of the pure polymer (c=0); and Tg(c) is the glass-transition of the polymer containing a dissolved penetrant at concentration c. Tg(c) can be estimated from the relation of Chow (14).

The derivation of eqns. (1) and (2) is described in ref. (6), which is attached. The derivation is based on the fact that the glass-transition temperature, Tg, of the polymer is depressed by the penetrant gas to an extent which depends on the penetrant concentration. The depression of Tg causes, in turn, a decrease in the gas solubility. The inflection point in the isotherm indicates the penetrant pressure (or concentration in the polymer) at which Tg is depressed to the temperature of the isotherm and a transition occurs from the glassy to the "rubbery" polymer state. At higher pressures (or concentrations) the solubility isotherm becomes linear because the solubility of many gases in rubbery polymers obeys Henry's law. At even

higher pressures (on concentrations) it is predicted that the isotherm will become **convex** to the pressure axis because of the plasticization of the polymer in its rubbery state.

It was shown previously that eqns. (1) and (2) describes very satisfactorily the dependence of the CO_2 solubility in poly(ethylene terephthalate), in blends of poly(vinylidene fluoride) and poly(methyl methacrylate), and in poly(vinyl benzoate), cf. ref (6) attached. During the past report period, the solubility of C_2H_6 in poly(ethyl methacrylate) [Tg(0) = 69°C] at 35.0°C and in poly (vinyl benzoate) [Tg(0) = 65°C] at 5.0°C was measured over a range of elevated pressures. The experimental data are shown in Figures 2 and 3. The solid curves in these figures were calculated from eqns. (1) and (2) in conjunction with the values of parameters S(0) and A listed in Table I. The agreement between theory and experiment is seen to be satisfactory. The experimental data for the C_2H_6/poly(vinyl benzoate) system at the highest experimental pressures exhibit a faster than linear increase in solubility (c) with increasing pressure, which suggests a strong plasticization of the polymer in the rubbery state.

It should be noted that these measurements are not complete and that more solubility data for the above C_2H_6/polymer systems are necessary to fully validate the new model. Solubility measurements with other gas/polymer systems are also necessary. The measurements are time-consuming because of the slow rates at which these systems approach solution equilibrium.

B. Gas Diffusivity

The above concepts can be extended to describe the **diffusion** of gases in glassy polymers for cases where the polymer is strongly plasticized (swelled) by the penetrant gas. It can be shown that the **temperature** dependence of the mutual diffusion coefficients for small molecules in polymers, D(T), can be expressed by the relation (7,15):

$$D(T) = D(T_o) / \alpha_T(T) , \tag{3}$$

where T is a specified temperature; T_O is a reference temperature; and α_T (T) is the "temperature shift factor" for relaxation times. It is suggested that the **concentration** dependence of diffusion coefficients can be expressed by a similar relation:

$$D(c) = D(0) / \alpha_T(c) , \tag{4}$$

where c is local concentration of the penetrant in the polymer; D(c) is the diffusion coefficient at concentration c; D(0) is the diffusion coefficient at infinite dilution ($c \rightarrow 0$); and $\alpha_T(c)$ is the "concentration shift factor" discussed in the previous section, cf. eqn. (2). Hence, eqns. (2) and (4) yield the relation:

$$D(c) = D(0) \exp \left\{ -A_D \left[\frac{Tg(c)\,[Tg(c) - Tg(0)]}{[Tg(0)]^2} \right] [\, Tg(0) - T \,] \right\} , \tag{5}$$

where all the symbols are as defined before. This equation is applicable to a specified constant temperature T and contains only two adjustable parameters, D(0) and A_D. These parameters can be determined by fitting eqn. (5) to experimental diffusion data for a range of penetrant concentrations in a polymer. Tg(0) can be determined by differential scanning calorimetry or thermomechanical analyses, and Tg (c) can be estimated from Chow's relation (14).

Figures 4 and 5 present a comparison of diffusion coefficients for CO_2 in poly(ethylene terephthalate) (PET) determined from the permeability and solubility data of Koros and Paul (16, 17) with the diffusion coefficients calculated from eqn. (5). The former diffusion coefficients were determined from the relation (2):

$$D(c_h) = \left[\bar{P}(p_h) + p_h \frac{d\bar{P}}{dp_h} \right] \left(\frac{dp}{dc} \right)_{p_h}, \qquad (6)$$

where $\bar{P}$ is a mean permeability coefficient; p_h is the pressure applied at the "upstream" (high-pressure) interface of a membrane in permeability measurements; and c_h is the penetrant concentration the polymer at that interface. The values of $d\bar{P}/dp_h$ are obtained from the dependence of $\bar{P}$ on p_h, and dc/dp is determined from the solubility isotherms.

Referring to Figures 4 and 5, it is seen that the values of D(c) calculated from eqn.(5) for the CO_2/PET system are entirely consistent with the values obtained from permeability and solubility measurements via eqn. (6), particularly when considering the combined experimental errors in these measurements. The parameters D(0) and A_D used in eqn. (5) are listed in Table II. It is interesting to note that eqn. (5) predicts an inflection in the D(c) versus c plot for the CO_2/PET system at 85°C and at c ≈ 4 cm^3 (STP)/cm^3 polym. However, more experimental data are required to confirm this inflection.

Figure 6 shows a similar comparison for CO_2 in polyarylate (PA) and polycarbonate (PC) at 35°C (18,19). The values of D(c) derived from experimental permeability and solubility data are in good agreement with the values obtained from eqn. (5) in conjunction with the parameters listed in Table III.

C. The Diffusion "Time-Lag"

Consider the permeation of a gas from a reservoir at a constant pressure p_h through a nonporous, homogeneous polymer membrane into another (finite) reservoir at a pressure p_l ($<<$ p_h). The period of time from the instant the gas contacts the membrane until the permeation

process reaches steady-state conditions is known as the "time-lag", L. Time-lags are related to diffusion coefficients, and the measurement of time lags is a common method of determining these coefficients (2-4). Thus, diffusion coefficients, D, can be determined from a solution of Fick's second law with the following initial and boundary conditions, which define the permeation process described above:

$$\frac{\partial c}{\partial t} = \frac{\partial}{\partial x}\left[D(c) \frac{\partial c}{\partial x} \right] \text{ in } 0 < x < \delta \, , \, t > 0 \, , \tag{7}$$

with

$$c(x,0) = 0 \qquad \text{for } x > 0$$

$$c(0,t) = c_h \qquad \text{for } t > 0$$

$$c(\delta,t) = 0 \qquad \text{for } t > 0$$

where c is the local penetrant gas concentration at a position coordinate x in the membrane; c_h is the concentration at the "upstream" (high-pressure) interface of the membrane in contact with the gas at pressure p_h; and δ is the membrane thickness. In this case $p_h >> p_l \approx 0$. When the diffusion coefficient is independent of concentration, i.e., $D(c) = D_0$, a constant, the asymptotic ($t \rightarrow \infty$) solution of eqn. (7) is:

$$L = \delta^2 / 6 D_0 \, ; \tag{8}$$

hence, D_0 can be calculated if L is known. However, the diffusion coefficients of gases in glassy polymers are strongly concentration-dependent (2-10). The relation between L and D(c) has been formulated for such cases by Frisch (20), cf. refs. (2-4):

$$L = \frac{\delta^2 \left\{ \int_0^{c_h} wD(w) \left[\int_w^{c_h} D(u)\, du \right] du \right\}}{\left[\int_0^{c_h} D(u)\, du \right]^3} \qquad (9)$$

where u and w are dummy variables. In order to solve eqn. (9) for the time-lag L it is necessary to know the exact functional dependence of D(c) on the penetrant concentration c. Accordingly, eqn. (9) was solved using the expression for D(c) derived from the concentration-temperature superposition model, i.e., from eqn. (5); the values of the time-lag L used in eqn. (9) were those reported by Barbari et al. (18,19) for CO_2 in polycarbonate at 35°C. This calculation yielded the values of parameters A_D and D(0) in eqn. (5). Next, knowing A_D and D(0), the diffusion coefficient D(c) was calculated as a function of c from eqn. (5) with the results shown by the solid curve in Figure 7. This curve is seen to be in excellent agreement with the values of D(c) calculated from eqn. (6) in conjunction with the permeability and solubility data of Barbari et al. (18, 19).

Further tests of the concentration-temperature superposition model using time-lag measurements with other penetrant/polymer systems and at various temperatures are necessary in order to validate the new model. It should be noted that the above procedure can also be used to **predict** diffusion time-lags if the parameters D(0) and A_D in eqn. (5) are known from other types of measurements [e.g., from D(c) determined from permeability and solubility data via eqn. (6)].

III. EFFECT OF INTRASEGMENTAL MOBILITY OF POLYMER CHAINS ON GAS PERMEABILITY

Control of the gas permeability and selectivity of polymer membranes has become a subject of strong research interest because of its importance for the development of new membrane separation processes. The ability to achieve such control demands a good understanding of the relationships between the chemical structure of polymers and their gas permeability. The objective of the study was to examine the effect of intrasegmental mobility on gas permeability of polyimide membranes. Polyimide membranes are being studied as potential membrane materials because of their high gas selectivity, good mechanical properties, and versatile chemistry.

The role of the intrasegmental mobility of polymer chains on the gas permeability and selectivity was brought to our attention by the observation that a polyimide containing a ***para***-phenyl diamine moiety in its backbone structure always has a higher gas permeability and a lower gas selectivity than its isomer with a ***meta***-phenyl diamine moiety. Examples of such a behavior is shown in Table IV for two types of polyimide isomers (21,22). It was speculated that the above differences are due to the fact that the ***para***-phenyl diamine chains of these polyimides can rotate around their principal axis whereas the ***meta***-phenyl diamine chains do not have a principal rotational axis, and therefore cannot rotate, cf. Figure 8 (1,3).

Accordingly, the intrasegmental mobility of PMDA - 3,3'-ODA and PMDA-4,4"-ODA polyimides was studied by dynamic mechanical analysis (DMA). The chemical structures of these polymers are shown in Figure 8. The DMA spectra shown in Figure 9 indicate that the polyimide with a ***para***-phenyl diamine moiety (PMDA-4,4'-ODA) (Tg = 400°C) has two sub-Tg transitions, at -80°C (peak 1) and 150°C (peak 2), whereas its ***meta*** isomer (PMDA-3,3'-ODA)

does not have any sub-Tg transitions in the DMA temperature range investigated (-120 to 260°C). The transition peak for PMDA-3,3'-ODA at 280°C (peak 3) corresponds to two glass-transitions (Tg), as found also by differential scanning calorimetry. The fact that the ***para*** isomer (PMDA-4,4'-ODA) exhibits two sub-Tg transitions, the lowest at -80°C, suggests that it possesses a measure of intrasegmental rotational mobility between -80°C and its glass-transition temperature (Tg = 400°C). By contrast, the ***meta*** isomer (PMDA -3,3'-ODA) exhibits no sub-Tg transitions, which indicates that rotational mobility is largely inhibited at temperatures below its Tg (=280°C).

These experimental results have been complemented by calculations of the torsional energies for the rotation of a single bond in PMDA-3,3'-ODA and PMDA-4,4'-ODA. The calculations were made in accordance with the method of Flory (23), with the results shown in Figure 9. This figure represents the computer simulation of intrasegmental rotational barriers of the ***para*** isomer PMDA-4,4'-ODA. As shown above, the DMA analysis indicates that only this isomer has rotational degrees of freedom, namely, the phenyl rings of its diamine moiety can rotate around the bonds with their dianhydride moieties, cf. Figure 10. It is seen that the rotation barrier between the rotation angles from 65° to 115° and from 245° to 295° is very small, ΔE = 0.08 kcal/mol. This small barrier can be overcome at relatively low temperatures. Hence, we suggest that this ΔE probably corresponds to peak 1 in Figure 8, which occurs at -80°C. By contrast, the rotation barrier between the rotation angles from 115° to 245°, ΔE = 6.5 kcal/mole, is probably too high for the phenyl ring to rotate freely at room temperature. However, this rotation can take place at higher temperatures, where the phenyl ring absorbs sufficient kinetic energy. Consequently the large rotation barrier, ΔE = 6.5 kcal/mole, probably

corresponds to peak 2 in Figure 8, which occurs at 150°C.

The above calculation indicates that the intrasegmental rotation of the phenyl rings in the diamine moieties of PMDA-4,4'-ODA is not entirely free. The rotation is clearly hindered by the rotation barriers between the rotation angles at 115° to 245°. This means that the phenyl rings probably ***vibrate*** between 65° to 115° and between 245° to 295°. Such vibrations will facilitate gas diffusion, and hence also gas permeation through PMDA-4,4'-ODA. Moreover, an increase in permeability commonly results in a decrease in the overall gas selectivity of the polymers.

The ***meta*** isomer, PMDA-3,3'-ODA, has no intrasegmental rotational degrees of freedom, as expected from its structure and indicated by the DMA analysis. Consequently, the gas permeability of this polymer is lower, and its gas selectivity higher, than that of its ***para*** isomer, PMDA-4,4'-ODA.

This study appears to be the first to provide direct evidence on the role of intrasegmental mobility of glassy polymers on their gas permeability and selectivity.

IV. PROPOSED WORK

A. The main effort during the following report period will be devoted to further tests of the new "concentration-temperature superposition principle" for the solution and diffusion of gases in selected glassy polymers. The following studies are proposed:

1) The solubility measurements now in progress will be completed and extended to other plasticizing gases and to different temperatures. More specifically, the solubility of C_2H_6 and C_3H_8 in poly(ethyl methacrylate) (PEMA) and poly(vinyl benzoate) (PVB) will be measured in

the temperature range from 5 to 45°C. These measurements will be made with a recording electromicrobalance over a pressure range sufficiently large to include the isothermal glass transition, i.e., the inflection in the solubility isotherms. The validity of the new solubility isotherm represented by eqns. (1) and (2) will be tested with these experimental data.

2) Diffusion "time-lags" will be measured for C_2H_6 and C_3H_8 in PEMA and PVB in the above temperature range and at several pressures in order to predict diffusion coefficients, D(c), for these gas/polymer systems via our new diffusion model, cf. eqns. (5) and (9). The predicted values of D(c) will be compared with values derived from independent permeability and solubility measurements, as discussed in Section II.B.

3) The concentration-temperature superposition principle will be extended to describe the pressure dependence of permeability coefficients for plasticizing gases in glassy polymers. In principle, this can already be done because the mean permeability coefficient, $\bar{P}$, can be expressed by the relation (1-4):

$$\bar{P} = \bar{D} \cdot S_h \, (for \, p_h >> p_l) \ , \tag{10}$$

where $\bar{D}$ is a mean diffusion coefficient defined by

$$\bar{D} = \int_{c_l}^{c_h} D(c) \, dc \, / \, (c_h - c_l) \tag{11}$$

and S_h (=c/p) is a solubility coefficient evaluated at pressure p_h; c is the concentration of the penetrant gas in a polymer membrane in solution equilibrium at pressure p; and subscripts *h* and *l* designate the "upstream" (high-pressure) and "downstream" (low-pressure) interfaces of a membrane in permeability measurements, respectively. S_h can be represented by eqns. (1) and

(2), while $\bar{D}$ can be obtained from eqn. (11) in conjunction with eqn. (5) for D(c). Substitution of these equations in eqn. (10) yields a complete expression for $\bar{P}$ as a function of penetrant pressure (or concentration in the polymer) for plasticizing penetrants. However, this expression is too complex for practical applications and must be simplified or an alternate expression for $\bar{P}$ must be found on the new model.

It should be noted that a variety of membrane separation processes involve gas mixtures containing components which plasticize the polymer membranes used. This is the case in the removal of CO_2 and H_2S from crude natural gas, the separation of CO_2 from mixtures with hydrocarbons in enhanced oil recovery, the dehydration of natural gas, etc. The new concepts developed in this study should prove very useful for membrane process design in such applications.

REFERENCES

1. S.A. Stern, Chapt. 1 in "Synthetic Membranes", M.B. Chenoweth, Ed., MMI Press Symposium Series, Vol. 5, Harwood Academic Publishers, NY, 1986, pp. 1-37.

2. W.J. Koros and R.T. Chern, Chapt. 20 in "Handbook of Separation Process Technology", R.W. Rousseau, Ed., Wiley-Interscience, New York, 1987, pp. 862-953.

3. S.A. Stern and H.L. Frisch, Ann. Revs. Mater. Sci., 11, 523 (1981).

4. H.L. Frisch and S.A. Stern, Crit. Revs. Solid State and Mater. Sci., 11(2), 123(1983), CRC Press, Boca Raton, FL.

5. S.A. Stern and S. Trohalaki, Chapt. 2 in "Barrier Polymers and Structures", ACS Symposium Series No. 423, American Chemical Society, Washington, D.C. 1990, pp. 22-59.

6. Y. Mi, S. Zhou, and S.A. Stern, Macromolecules, 24, 2361 (1991).

7. J.D. Ferry, "Viscoelastic Properties of Polymers", 34d Ed., J. Wiley and Sons, New York, 1980.

8. W.R. Vieth, J.M. Howell, and J.H. Hsieh, J. Membrane Sci., 1, 177 (1976).

9. D.R. Paul and W.J. Koros, J. Polym. Sci., Polym. Phys. Ed., 14, 675 (1976).

10. W.J. Koros and D.R. Paul, J. Polym. Sci:, Polym. Phys. Ed., 16, 1947 (1978).

11. D.R. Paul, Ber. Bunsenges, Phyts. Chem., 83, 294 (1979).

12. W.J. Koros, D.R. Paul, and G.S. Huvard, Polym., 20, 956 (1974).

13. W.R. Vieth, Chapts. 2 and 3 in "Membrane Systems: Analysis and Design", Hanser Publishers, New York, 1989, pp. 9-66.

14. T.S. Chow, Macromolecules 13, 362 (1980).

15. S. Chen and J.D. Ferry, Macromolecules 1, 270 (1968).

16. W.J. Koros and D.R. Paul, J. Polym. Sci., Polym. Phys. Ed., 16, 1947 (1978); ibid, 16, 2171 (1978).

17. W.J. Koros, Ph.D. Dissertation, Dept. of Chemical Engineering, The University of Texas at Austin, 1977.

18. T.A. Barbari, W.J. Koros, and D.R. Paul, J. Membrane Sci., **42**, 69 (1989).

19. T.A. Barbari, Ph.D. Dissertation, Dept. of Chemical Engineering, The University of Texas at Austin, 1986.

21. S.A. Stern, Y. Mi, H. Yamamoto, and Anne K. St. Clair, J. Polym. Sci.: Part B: Polym. Phys., **27**, 1887 (1989).

22. W.J. Koros, Polym. J., **23**, 481 (1991).

20. H.L. Frisch, J. Phys. Chem., **61**, 93 (1957).

23. P.J. Flory, "Statistical Mechanics of Chain Molecules", Interscience, New York 1969.

TABLE I

VALUES OF MODEL PARAMETERS IN EQNS (1) AND (2) FOR CO_2 IN TWO GLASSY POLYMERS

Polymer	S(0)	A_S
PEMA[a]	5.1841	0.27046
PVB[b]	2.5169	0.01059

[a] at 35°C; [b] at 5°C

Units: S(0) [cm^3(STP)/(cm^3.polym.atm)], A $(°K)^{-1}$

PEMA = Poly(ethyl methacrylate), PVB = Poly(vinyl benzoate)

TABLE II

VALUES OF MODEL PARAMETERS IN EQN. (5) FOR CO_2 IN POLY(ETHYLENE TEREPHTHALATE)

Temperature, t	D(0)	A_D
25	0.3474	0.7379
35	0.8437	0.7372
45	1.3261	1.0824
55	2.4929	1.4327
65	4.3272	1.9864
75	8.8245	2.2695
85	15.883	6.1773

Units: D(0) [cm^2/s] × 10^9, A_D $(°K)^{-1}$; t (°C)

TABLE III

VALUES OF MODEL PARAMETERS IN EQN. (5) FOR CO_2 IN TWO GLASSY POLYMERS AT 35°C

Polymer	D(0)	A_D
PA	7.0125	0.2869
PC	13.7125[a]	0.1897[a]
	14.3325[b]	0.1813[b]

[a] Calculated from eqn. (5) using the diffusivity data of Barbari et al. [18,19]

[b] Calculated from eqn. (9) using the time-lag data of Barbari et al. [18,19]

Units: D(0) [cm^2/s] $\times$ 10^9, A_D $(°K)^{-1}$

PA = Polyarylate, PC = Polycarbonate

TABLE IV

PERMEABILITY AND SELECTIVITY OF POLYIMIDE ISOMERS TO DIFFERENT GASES AT 35.0°C

Gas Permeability

Polymer	$\bar{P}(CO_2)x10^{10}$	$\bar{P}(CH_4)x10^{10}$	$\bar{P}(O_2)x10^{10}$	$\bar{P}(N_2)x10^{10}$
6FDA-4BDAF	19.0	0.51	5.40	0.95
6FDA-3BDAF	6.30	0.13	1.35	0.23
PMDA-4,4′-ODA	1.14	0.026	0.22	0.047
PMDA-3,3′-ODA	0.50	0.0080	0.13	0.020

Gas Selectivity

Polymer	$\alpha^*(CO_2/CH_4)$	$\alpha^*(N_2/CH_4)$	$\alpha^*(O_2/N_2)$	$\alpha^*(H_2/CH_4)$
6FDA-4BDAF	37	1.9	5.5	34
6FDA-3BDAF	48	1.8	5.6	156
PMDA-4,4′-ODA	43	1.8	4.5	115
PMDA-3,3′-ODA	62	2.5	7.2	450

Units: Mean permeability coefficient, $\bar{P}$ [cm^3(STP)·cm/(s·cm^2·cmHg)];
Pressure difference across membrane, Δp = 100 psig (6.8 atm);

Selectivity, $\alpha^*(A/B) = \bar{P}(A)/\bar{P}(B)$.

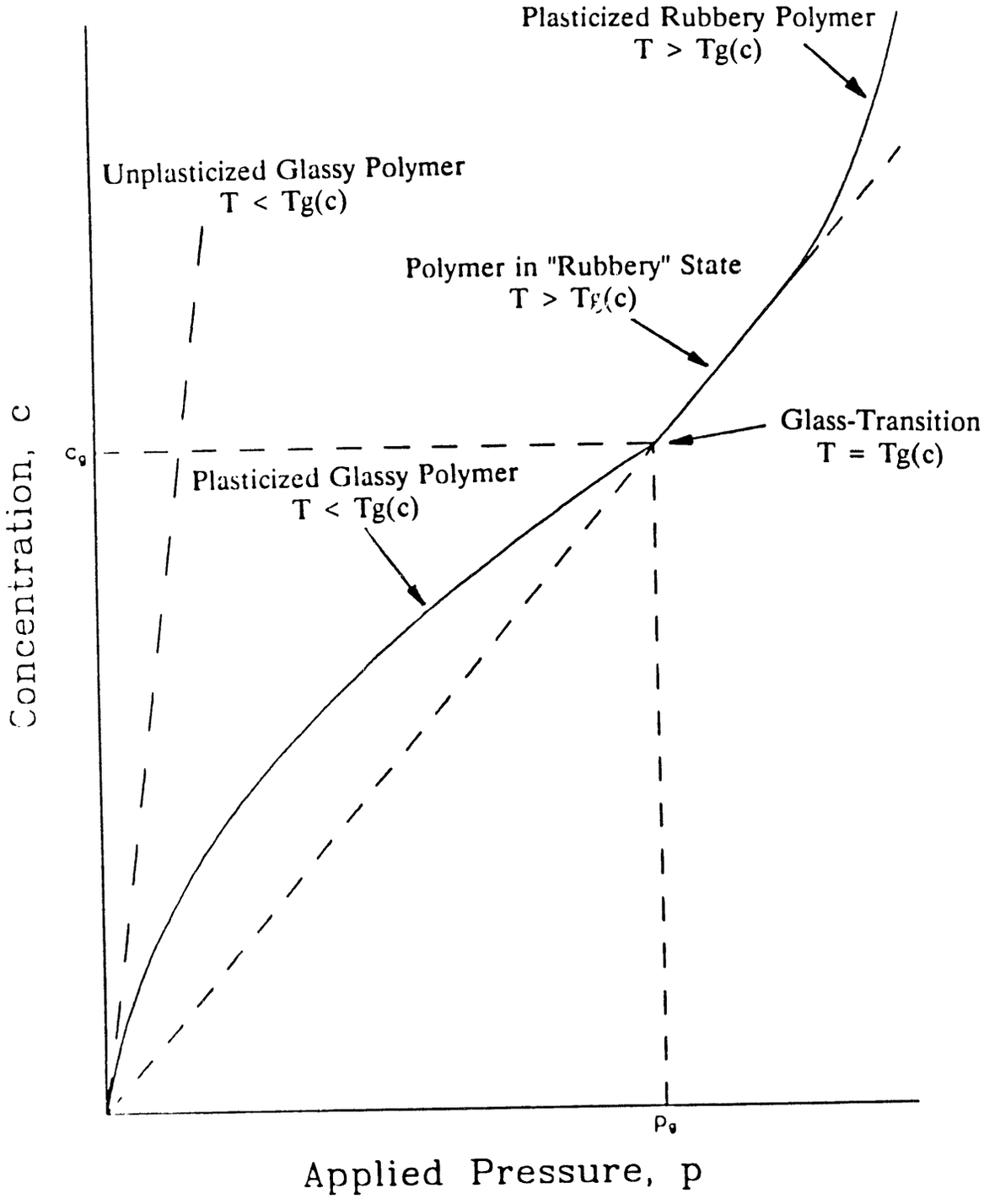

Figure 1. **Typical solubility isotherms for plasticizing gases in glassy polymers. All isotherms are for the same temperature.**

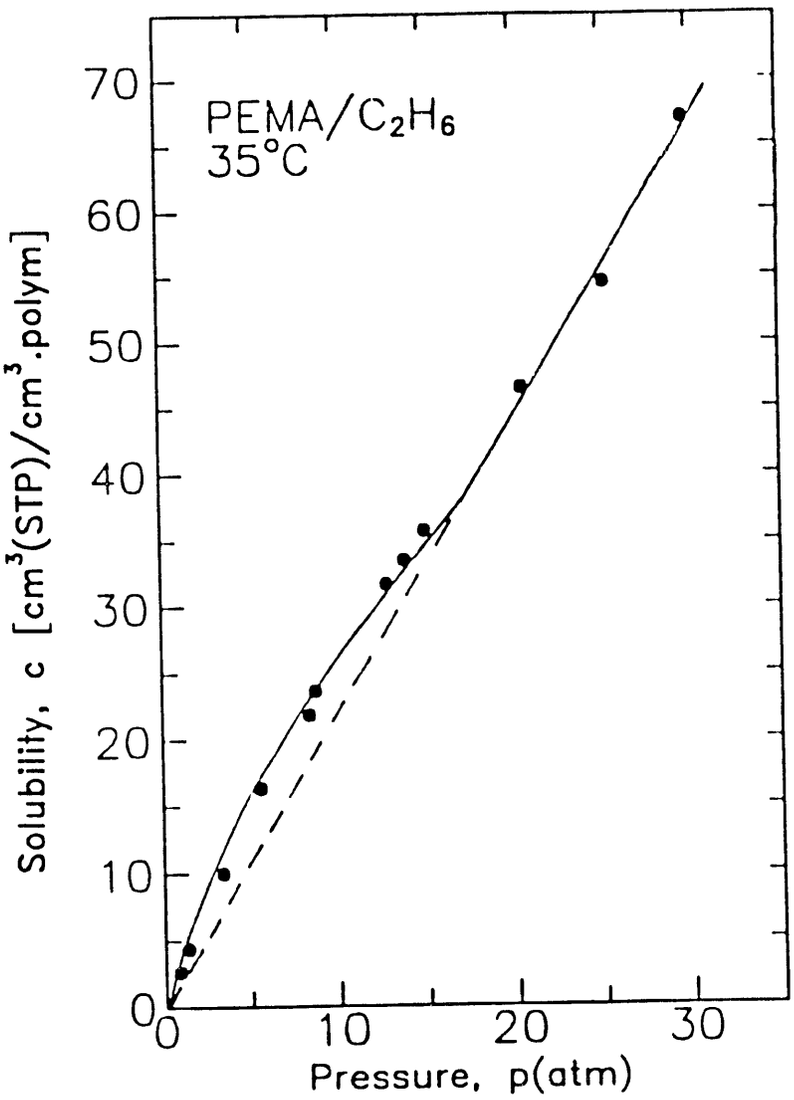

Figure 2. **Solubility isotherm for C_2H_6 in poly(ethyl methacrylate) at 35°C.**

The solid curve was calculated from eqns 1 and 2 in conjunction with the parameters listed in Table I

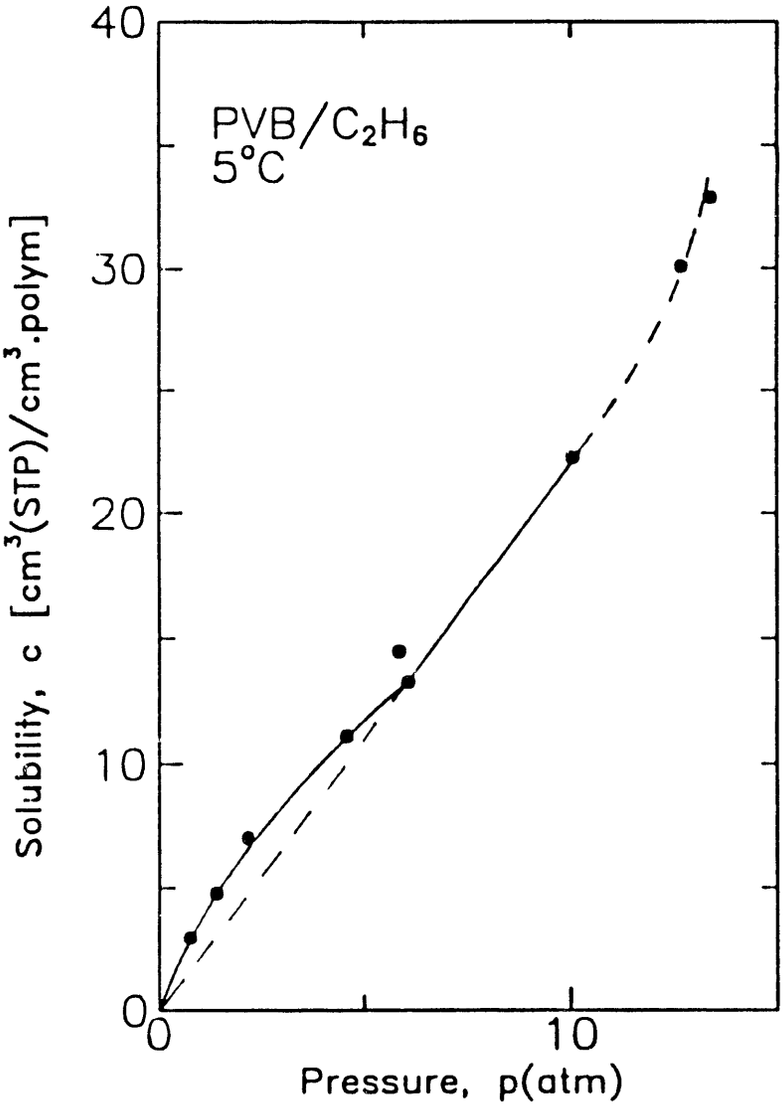

Figure 3. Solubility isotherm for C_2H_6 in poly(vinyl benzoate) at 5°C.

The solid curve was calculated from eqns 1 and 2 in conjunction with the parameters listed in Table I.

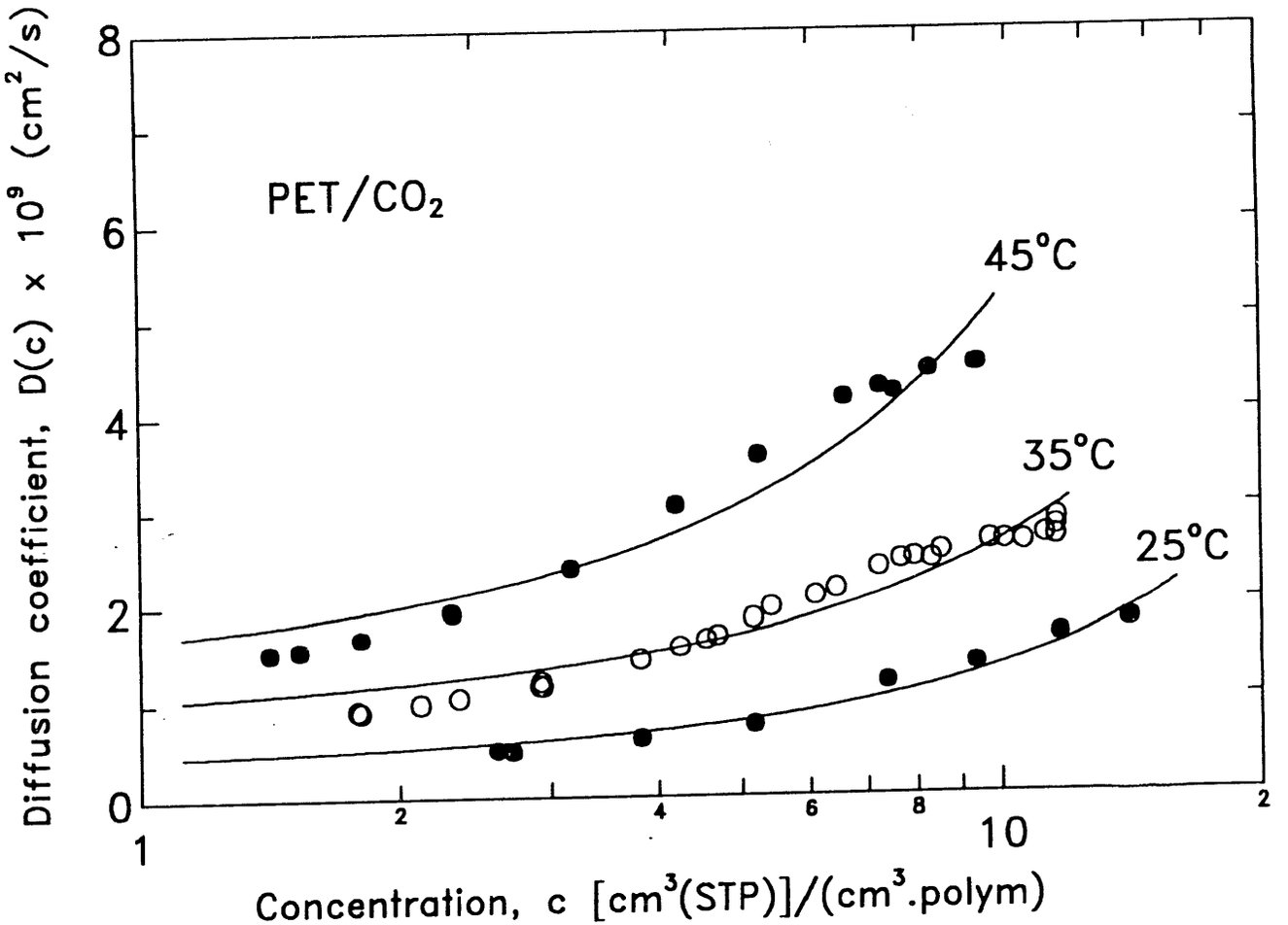

Figure 4. Diffusion Coefficients for CO_2 in poly(ethylene terephthalate) (PET) at different temperatures.

The solid curves drawn through the data points were calculated from eqn. (5) in conjunction with the parameters listed in Table II, whereas the data points were calculated from eqn. (6) and the permeability and solubility measurements of Koros et al. [16,17]

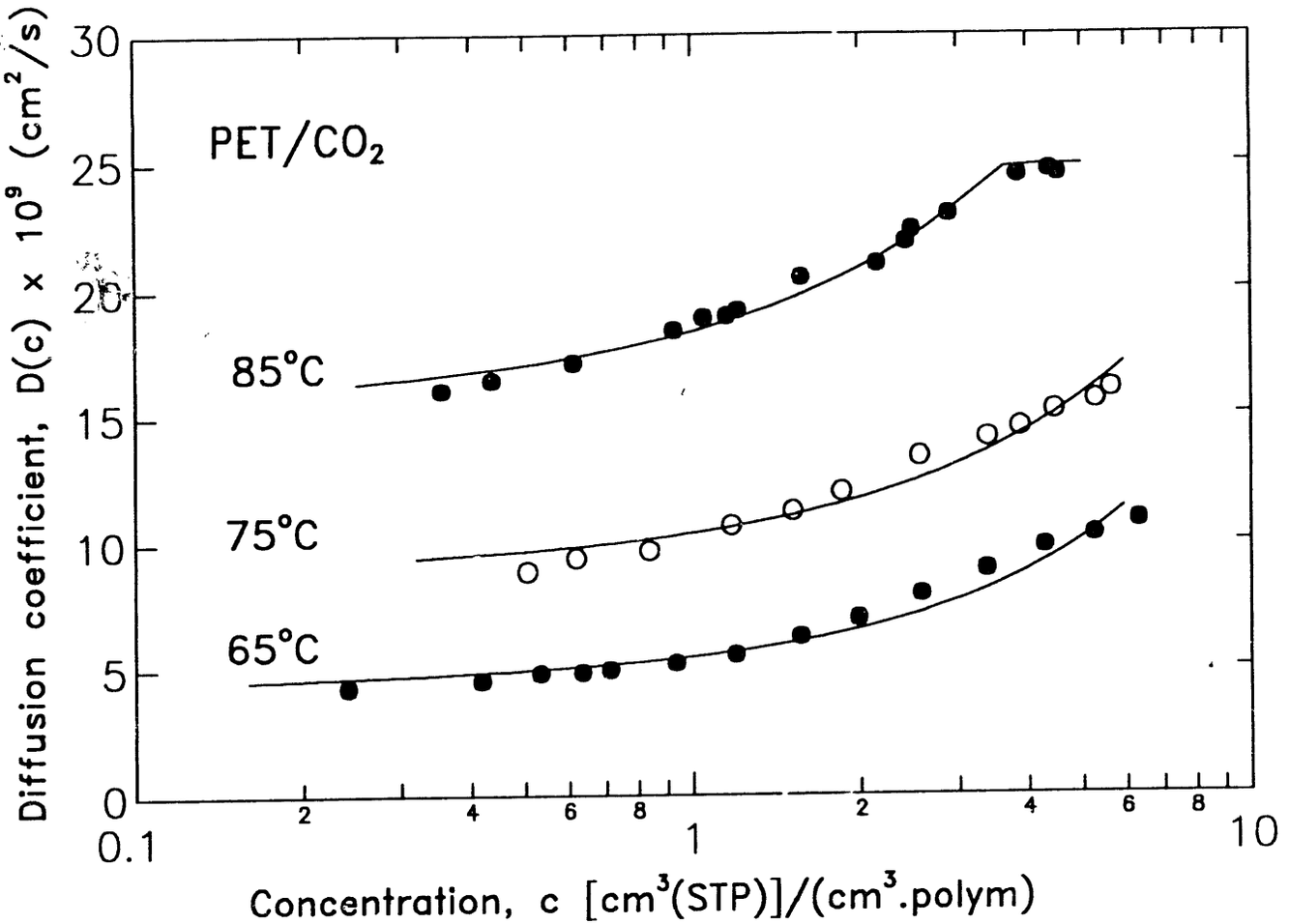

Figure 5. Diffusion Coefficients for CO_2 in poly(ethylene terephthalate) (PET) at different temperatures.

The solid curves drawn through the data points were calculated from eqn. (5) in conjunction with the parameters listed in Table II, whereas the data points were calculated from eqn. (6) and the permeability and solubility measurements of Koros et al. [16,17]

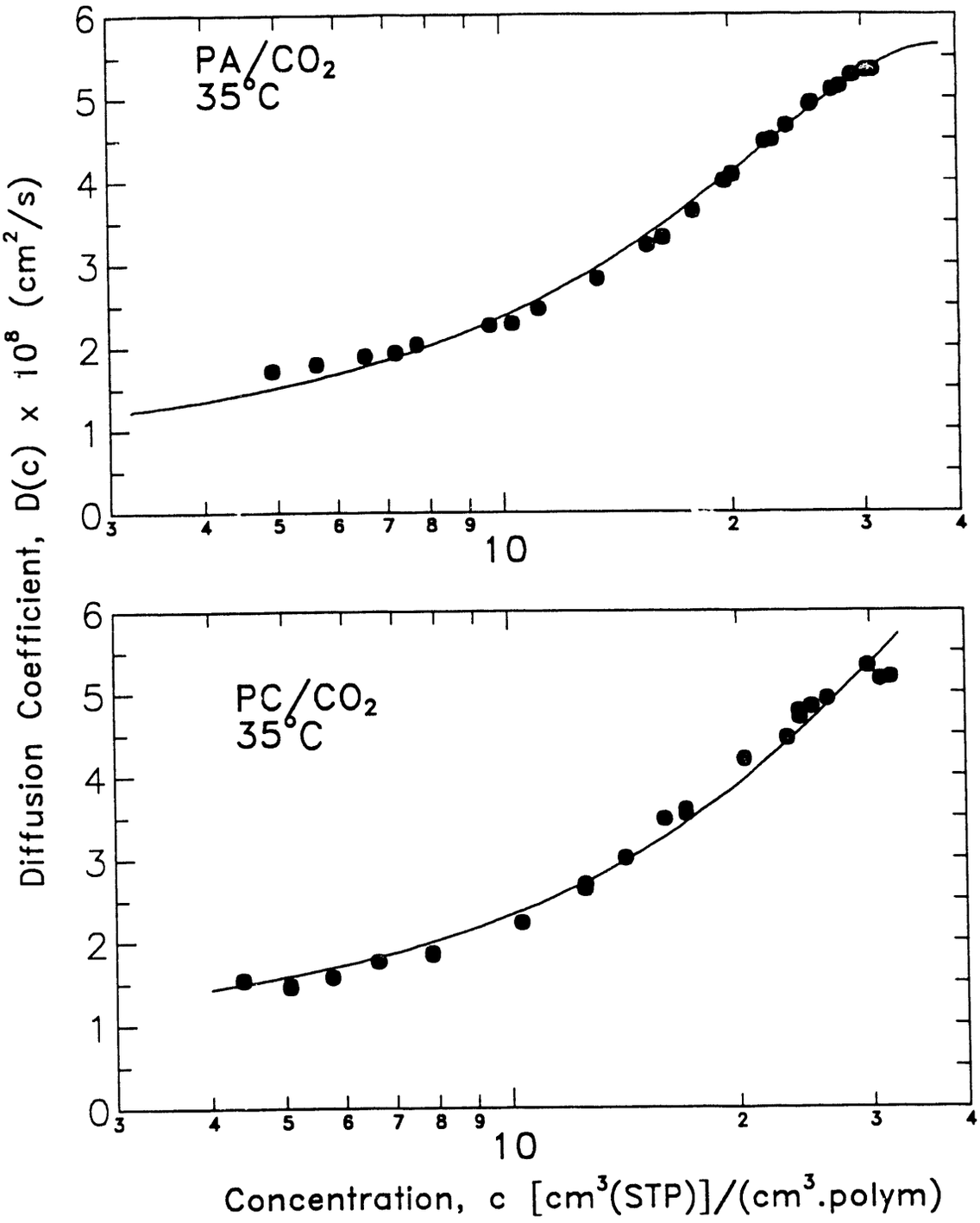

Figure 6. Diffusion coefficients for CO_2 in polyarylate (PA) and polycarbonate (PC) at 35°C.

The solid curves drawn through the data points were calculated from eqn. (5) in conjunction with the parameters listed in Table III, whereas the data points were calculated from eqn. (6) and the permeability and solubility measurements of Barbari et al. [18,19]

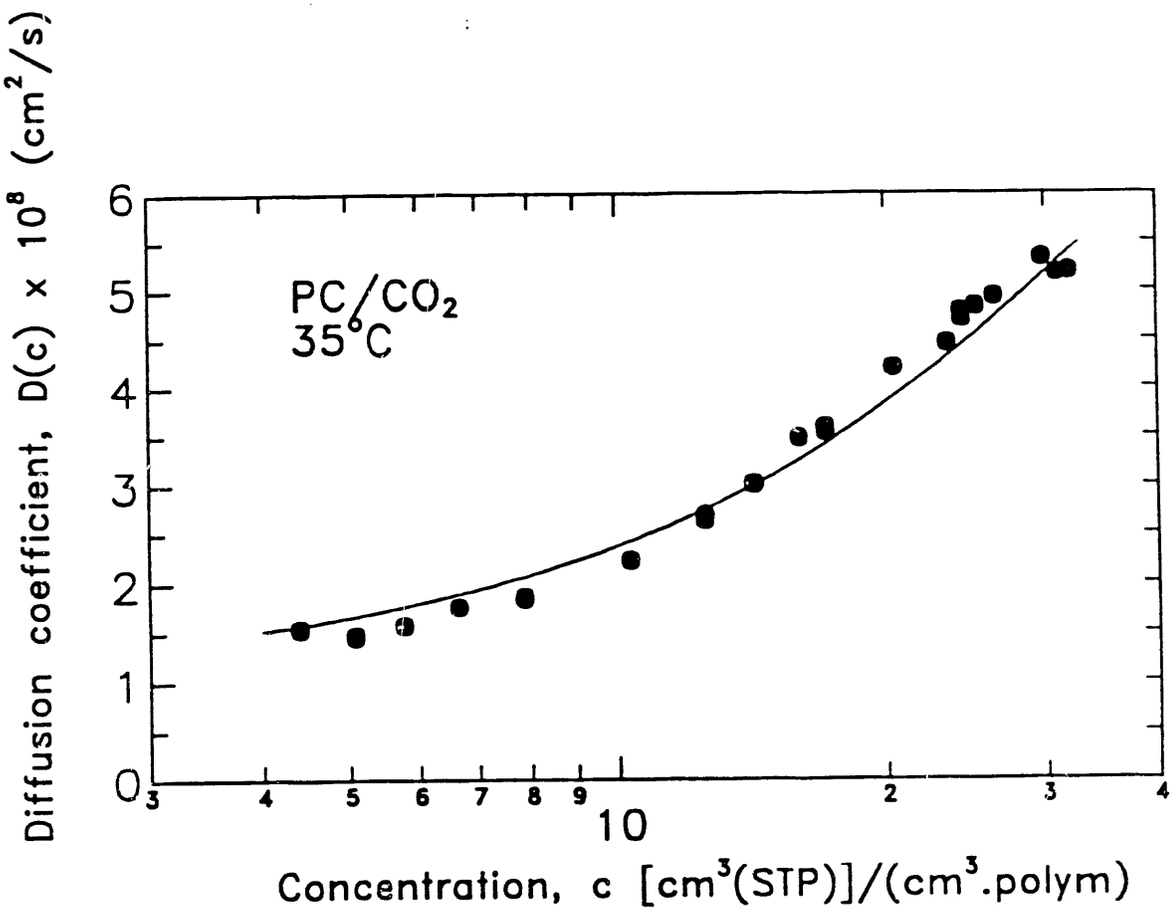

Figure 7. Prediction of the diffusion coefficient as a function of concentration for CO_2 in polycarbonate at 35°C from time-lags.

The solid curve was calculated from eqn. (5) using parameters A_D and D(0) determined from eqn. (9) [A_D=0.1813, D(0)=1.433 x 10^{-8} (cm^2/s)]. The experimental values of D(c) (full circles) were calculated from eqn. (6) using the data of Barbari et al. [18,19]

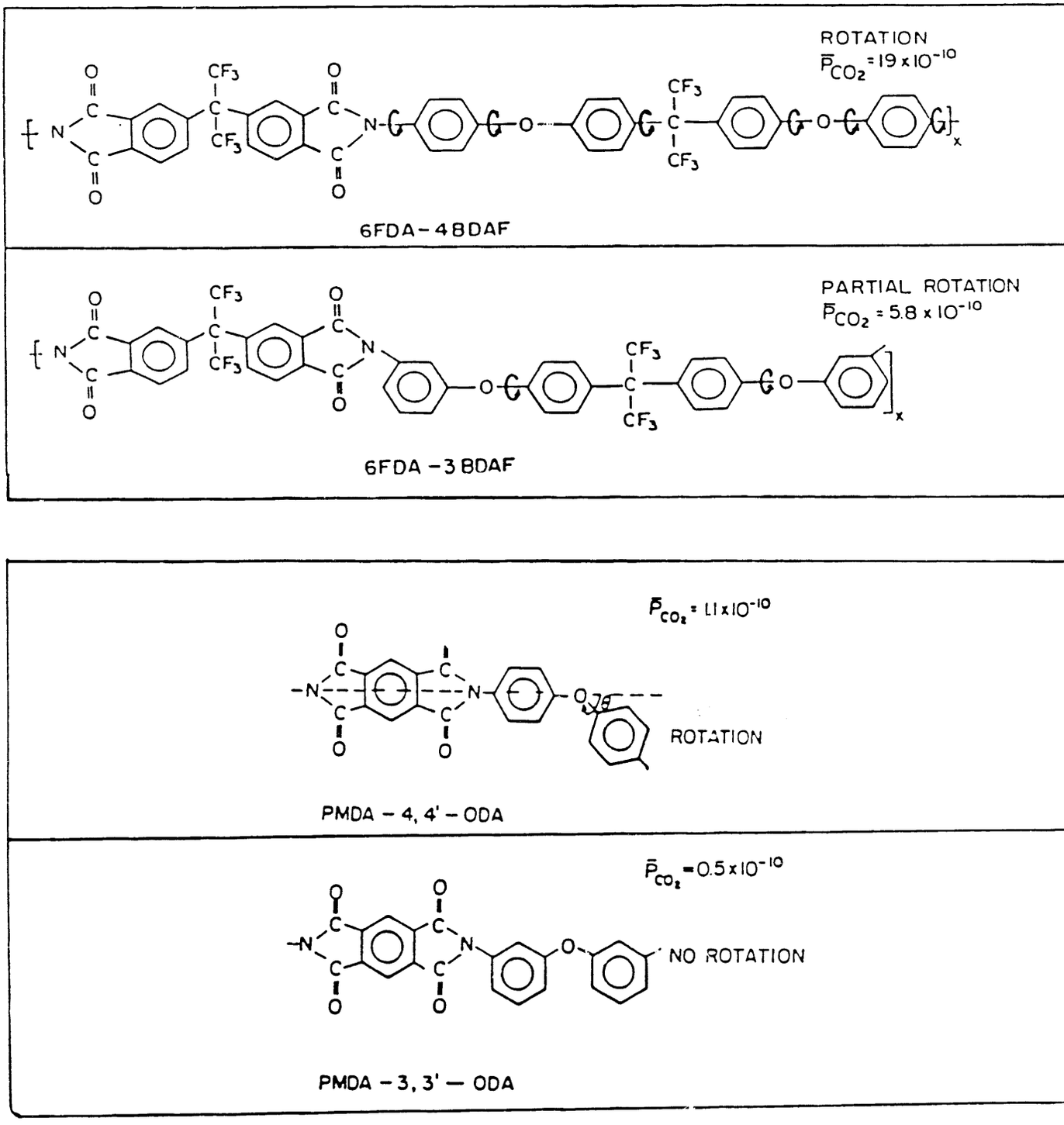

Figure 8. Intrasegmental rotational mobility in polyimide isomers.

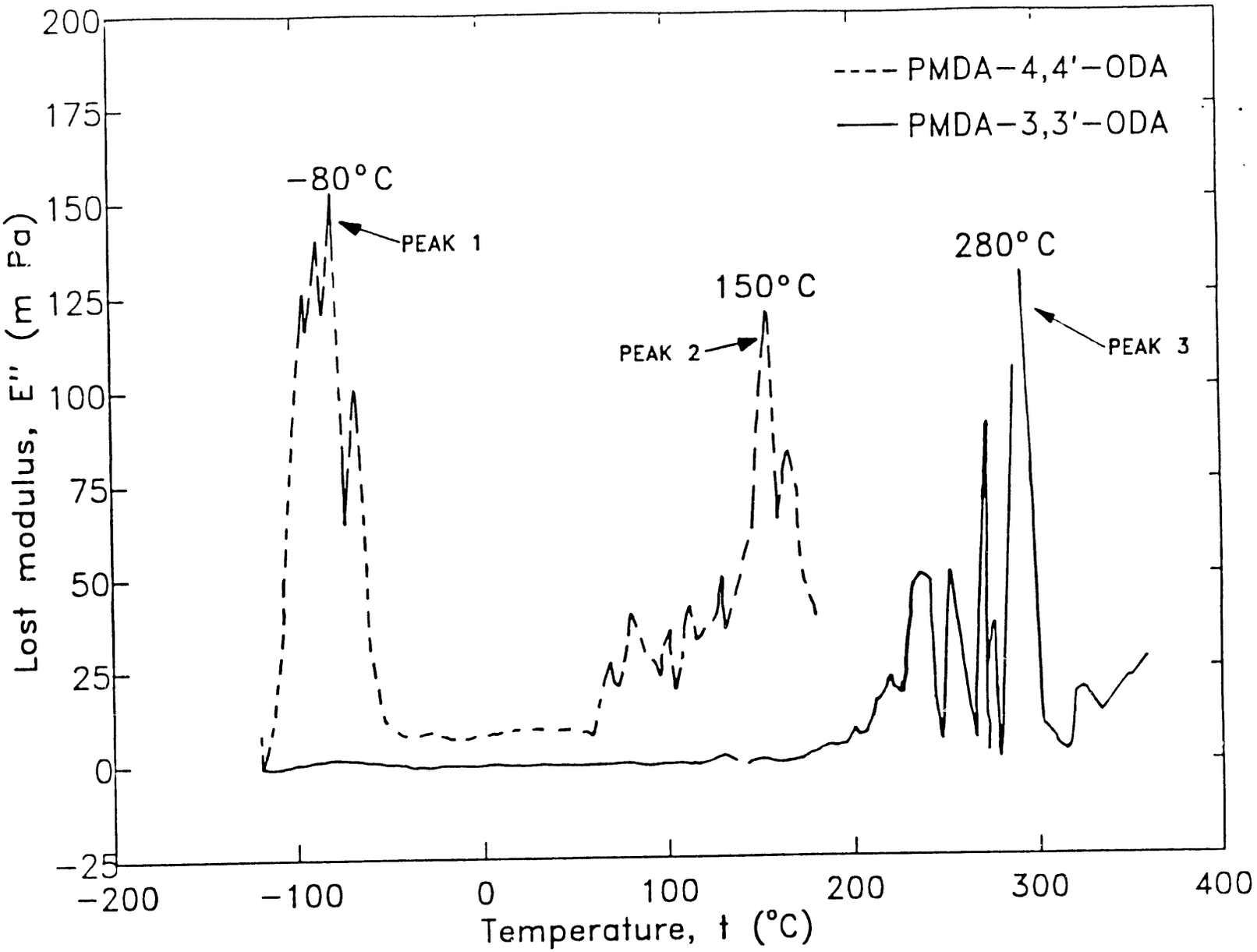

Figure 9. Temperature spectrum of PMDA-4,4'-ODA and PMDA-3,3'-ODA by dynamic mechanical analysis (DMA).

Peak 1: Vibration peak of 4,4'-phenyl ring around its principal axis.

Peak 2: Free rotation peak of 4,4'-phenyl ring around its principal axis.

Peak 3: Glass-transition peak of PMDA-3,3'-ODA.

PMDA-3,3'-ODA has no sub-T_g transition ($T_g \approx 280°C$) indicating very low intrasegmental mobility, as expected from structure. PMDA-4,4'-ODA has two sub-T_g transitions ($T_g \approx 400°C$) indicating intrasegmental mobility above -80°C.

Rotation of Bonds in Diamine Moiety of Polyimides

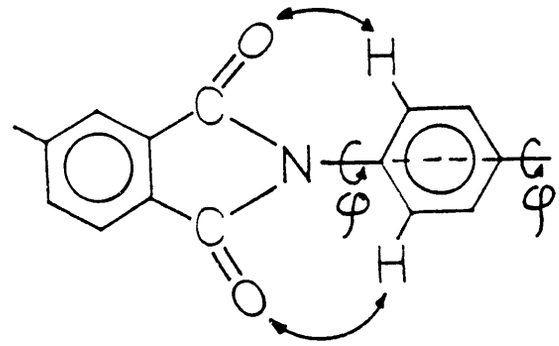

where φ is the angle of rotation of a single bond around its principal axis.

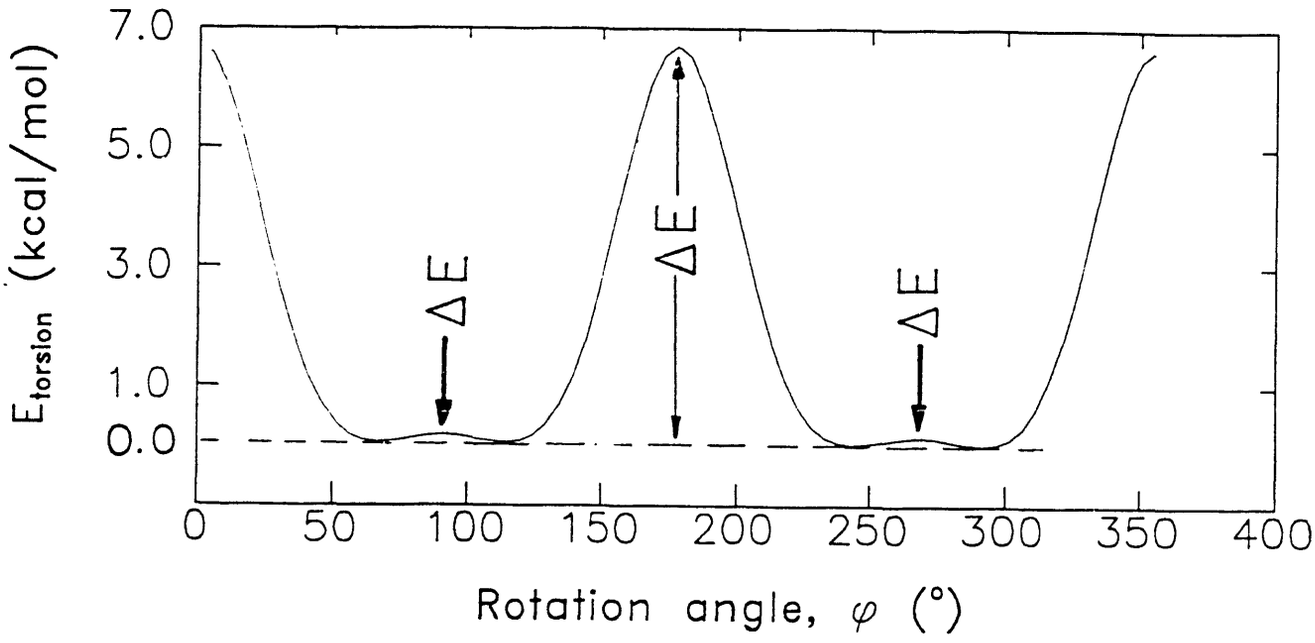

Figure 10 Torsional energy of nonbonded atoms between C=O and H-C_{phenyl} groups in diamine moiety of PMDA-4,4'-ODA.

This figure shows that the phenyl ring of the diamine is free to rotate only in the angle range from 65° to 115° and from 245° to 295°. The barrier between 65° and 115° and/or between 245° and 295° is very small and probably corresponds to peak 1 in Figure 8. The large rotational barrier between 150° and 245° probably corresponds to peak 2 in Figure 8.

END

DATE FILMED

01/22/92